Optimal Chandra/XMM-Newton band-passes for detecting low temperature groups and clusters of galaxies

Caleb Scharf

Columbia Astrophysics Laboratory, Columbia University, MC5247, 550 West 120th St., New York, NY 10027, USA.

caleb@astro.columbia.edu

ABSTRACT

In this short paper I present the results of a calculation which seeks the maximum, or optimal, signal-to-noise energy band for galaxy group or cluster X-ray emission detected by the Chandra and XMM-Newton observatories. Using a background spectrum derived from observations and a grid of models I show that the "classical" 0.5-2 keV band is indeed close to optimal for clusters with gas temperatures > 2 keV, and redshifts $z < 1$. For cooler systems however, this band is generally far from optimal. Sub-keV plasmas can suffer 20-60% signal-to-noise loss compared to an optimal band, and worse for $z > 0$. The implication is that current and forthcoming surveys should be carefully constructed in order to minimize bias against the low mass, low temperature end of the cluster/group population.

Subject headings: Xrays:galaxies:clusters—methods:data analysis

1. Introduction

The X-ray emission from $10^6 - 10^8$K plasma in the gravitational potentials of massive clusters and groups of galaxies has proved to be an invaluable means by which these systems can be robustly detected and quantified, e.g. Gioia et al. (1990). The use of all- or partial-sky X-ray data (Ebeling et al. 1997; Henry et al. 1992; Gioia et al. 1990) and archival pointed data (Rosati et al. 1995; Scharf et al. 1997; Vikhlinin et al. 1998) in constructing statistically complete catalogs of clusters and groups has dramatically filled in our picture of their evolution, from low redshifts to $z \sim 1$ (Borgani et al. 2001). The new Chandra and XMM-Newton observatories promise to further extend this early work, and in combination with measurements of the Sunyaev Z'eldovich (S-Z) CMB decrement, will allow us to refine

and extend our use of clusters as tools for cosmology (Haiman, Mohr, & Holder 2001). At the lower end of the mass scale, Chandra and XMM-Newton will permit the poorer, lower luminosity clusters and groups (systems with temperatures < 2 keV) to be systematically detected for the first time to redshifts of a few tenths. Previous surveys for these systems have often had to rely on prior optical catalogs, complicating the estimation of statistical completeness and bias (Mulchaey & Zabludoff 1998).

A common aspect of X-ray group and cluster surveys has been the frequent (although not universal) choice of a pass-band from 0.5-2keV. Such a band typically helps minimize the contribution of soft Galactic emission, and harder particle background, while maximizing sensitivity to general cluster emission (McHardy et al. 1998; Rosati et al. 1995). Previous imaging X-ray observatories have also not had the good spectral resolution of Chandra or XMM-Newton, so the choice of band was less controllable.

In this short paper I present a set of simple calculations aimed at determining a set of optimal pass-bands for thermal plasmas over a range of temperatures and redshifts. I also demonstrate the relationship to the commonly used 0.5-2 keV band, and argue that future surveys of cooler systems must take the band-pass explicitly into account, or risk seriously biasing their estimates of the space density of such systems.

2. Optimal energy bands

The signal-to-noise criterion I use here is $S/\sqrt{N}$, where S is the source photon count, N is the appropriate background count. This is chosen as a decent approximation to the various forms of detection significance criteria used in X-ray surveys for extended sources. Typically, a mean background count per sky area is estimated, and the deviation of the count rate in a given area, minus the background, is compared to the statistical (usually Poisson) fluctuation in the background over that area.

2.1. The calculations

A typical background spectrum is derived across the full instrument band-pass by combining high Galactic latitude data ($< nH >\sim 1 \times 10^{21}$) in which bright sources and periods of high particle background (flares) have been removed. For Chandra, the data was culled by combining archival fields and the online background data. Similarly, for XMM, archival PV data and online background data was utilized. The background spectrum is derived by binning photons from the entire field-of-view and performing a simple, linear, sliding window

smoothing over 5 PI channels. The spectra so derived are still somewhat noisy, but not at a level which alters the results presented here.

A grid of models is generated across a range of temperatures and redshifts using XSPEC, with a MEKAL plasma, 1/3rd Solar abundances, $< nH >$ is set to a high Galactic latitude maximum of $1 \times 10^{21}\mathrm{cm}^2$, and the results are robust to reasonable variations in these quantities. Δz is set to 0.1 and kT is actually set over a range from 0.1 to 12.9 keV in steps of 0.1 keV, although only temperatures of 0.2, 0.5, 1.0, 2.0, 4.0, and 6.0 keV are presented here. The spectra are then forward-folded through the on-axis RMF's and ARF's for the respective instruments. In the case of the Chandra front-illuminated CCD device (ACIS-I), off-axis responses are also used in an effort to evaluate the effect of radiation damage induced charge-transfer inefficiencies (CTI) (see §2.2 &3). All Chandra responses used here assume that basic CTI corrections have beeen applied to the data (e.g. Townsley et al. (2000)). The corrections reduce the position dependence (on the chips) of the gain and grade distributions (which distort the inferred photon energies), but an energy and position dependent degradation of spectral resolution remains.

An unrestricted search is then made for the maximal signal-to-noise by varying the lower (E_1) and upper (E_2) energy bands independently, as a function of z.

2.2. The results

Figures 1,2,3, and 4 present the optimal band search results for, respectively, the Chandra ACIS-I, ACIS-S, the XMM-Newton MOS, and PN instruments.

Some of the energy band limits show clear features as a function of redshift, however these all correspond to small variations in actual signal-to-noise, as is reflected by the smoothness of the 0.5-2 keV to optimal ratio curves. The features are due to the combination of the shape of the instrumental response and features in the background and source spectra. For example, in Figure 2, the upper limit band pass curve for $kT = 6$ keV (heaviest line) exhibits a sharp drop as the spectrum redshifts from $z = 0.6$ to 0.7. This is entirely due to the location of a flourescent Si K-α line (at ~ 1.7 keV) in the background, from reflection in the Chandra mirror assembly. As the redshift of the source increases a critical point is reached where the optimal band edge crosses this background line, and the optimum jumps to a lower energy.

The key results may be summarized as follows. For all instruments, plasmas with $kT < 2$ keV have optimal bands which differ significantly from the 0.5-2 keV bandpass. For the coolest plasma considered here (0.2 keV, 2.3×10^6 K) at $z = 0.1$ the 0.5-2 keV band

suffers a 55-65% S/N loss with Chandra, and a $\sim 45\%$ S/N loss with XMM compared to the optimal band pass. The optimal band in this case has a maximum range from $0.4 - 0.7$ keV for Chandra and $0.4 - 0.8$ for XMM, both of which are very narrow. At higher redshifts the S/N loss for the 0.5-2 keV band increases significantly. As the plasma temperature increases the optimal band rapidly widens. For a 1 keV plasma at $z = 0.1$ the optimal bands are in the range of $0.6 - 1.2$ keV, and have a S/N only 10% better than 0.5-2 keV, although this typically increases with redshift. The results for a 6' off-axis response function for the Chandra ACIS-I instrument, with a lower CCD row number and hence smaller CTI, are very similar to the high row number, on-axis calculations. Variations in band limits between the two are $\leq 5\%$, and therefore negligible.

In a survey, where the space density is to be recovered, the effective volume in which a source of a given intrinsic luminosity can be detected, is calculated based on the maximal redshift of detectability. A 10% drop in S/N compared to that expected propagates into a $\sim 10\%$ error in volume, consequently the band corrections suggested here are critical.

3. Conclusion

With luminosities of 10^{41-43}erg s^{-1}, low mass, cool ($kT < 2$ keV) groups and clusters of galaxies will form a significant fraction of the extended emission X-ray systems detectable to $z \sim 0.5$ in medium-deep Chandra and XMM exposures. Probing this population of collapsed systems is vital for improving our understanding of both the overall cluster mass function and the regime where gravitational collapse and astrophysical energies are comparable (Lloyd-Davies, Ponman, & Cannon 2000).

I have demonstrated here that the choice of band-pass is critical in both maximizing the detection sensitivity for clusters, and in its correct quantification in order to recover the true space density of poor cluster systems. The optimal bands presented here can serve as a reference point for Chandra and XMM surveys.

For the radiation damaged ACIS-I on Chandra, once the data is processed to correct for much of the CTI effect (e.g. Townsley et al. (2000)) the impact of the reduced spectral resolution on the optimal band limits is minimal (similarly for the inherent CTI in the back illuminated chips), and $\leq 5\%$ in amplitude at all energies. It appears that it can therefore be safely ignored in this situation.

It has been assumed here that cluster emission is isothermal. In reality this is often not the case, and significant temperature structure or gradients are present in massive clusters, and are likely also in lower mass systems. This will further complicate not only the absolute

detection of a cluster, but could bias the estimation of flux in a single band. In a future work (Scharf, in preparation) I will discuss the more complex issues involved with X-ray and S-Z detection biases for clusters in the context of their use as cosmological probes.

CAS gratefully acknowledges helpful discussions with D. Helfand and F. Paerels and the generous support of the Columbia Astrophysics Laboratory for this work.

REFERENCES

Borgani, S. et al. 2001, ApJ, 561, 13

Ebeling, H., Edge, A. C., Fabian, A. C., Allen, S. W., Crawford, C. S., & Boehringer, H. 1997, ApJ, 479, L101

Gioia, I. M., Henry, J. P., Maccacaro, T., Morris, S. L., Stocke, J. T., & Wolter, A. 1990, ApJ, 356, L35

Haiman, Z., Mohr, J. J., & Holder, G. P. 2001, ApJ, 553, 545

Henry, J. P., Gioia, I. M., Maccacaro, T., Morris, S. L., Stocke, J. T., & Wolter, A. 1992, ApJ, 386, 408

Lloyd-Davies, E. J., Ponman, T. J., & Cannon, D. B. 2000, MNRAS, 315, 689

McHardy, I. M. et al. 1998, MNRAS, 295, 641

Mulchaey, J. S. & Zabludoff, A. I. 1998, ApJ, 496, 73

Rosati, P., della Ceca, R., Burg, R., Norman, C., & Giacconi, R. 1995, ApJ, 445, L11

Scharf, C. A., Jones, L. R., Ebeling, H., Perlman, E., Malkan, M., & Wegner, G. 1997, ApJ, 477, 79

Townsley, L. K., Broos, P. S., Garmire, G. P., Nousek, J. A. 2000, ApJ, 534, 139

Vikhlinin, A., McNamara, B. R., Forman, W., Jones, C., Quintana, H., & Hornstrup, A. 1998, ApJ, 502, 558

Fig. 1.— Results of an optimal band search for the Chandra ACIS-I FI chip array. Left panel (a): Upper (solid) and lower (dashed) energy band limits (E_2 and E_1) are plotted as a function of redshift (z). Plasma temperatures are 0.2 keV (lightest weight curves), 0.5 keV, 1 keV, 2 keV, 4 keV, and 6 keV (heaviest curves). Right panel (c): The ratio of signal-to-noise in the classical 0.5-2 keV band to that in the optimal band is plotted (as a percentage) versus redshift for the 6 plasma temperatures.

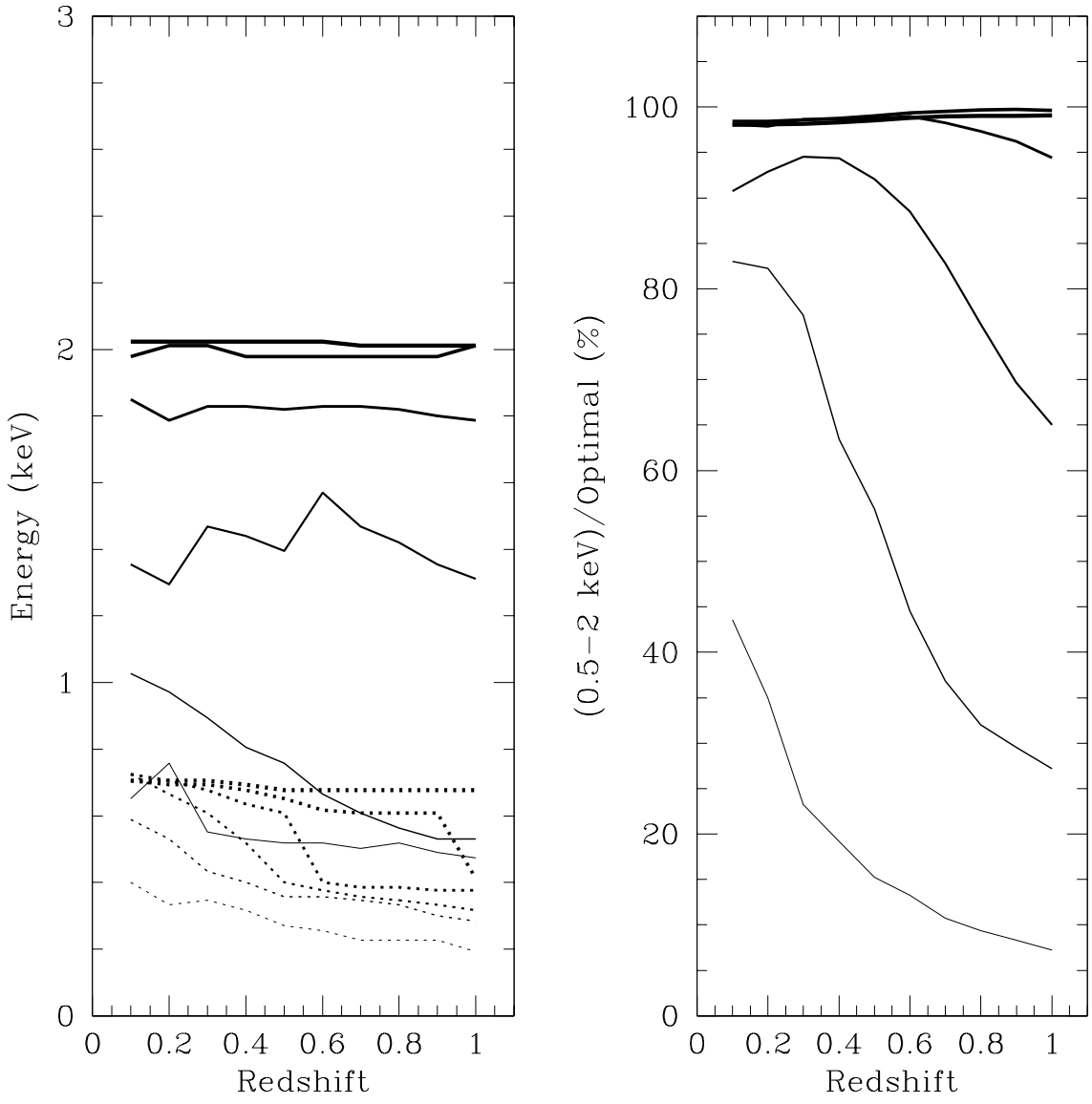

Fig. 2.— As for Figure 1, for the Chandra ACIS-S BI chips

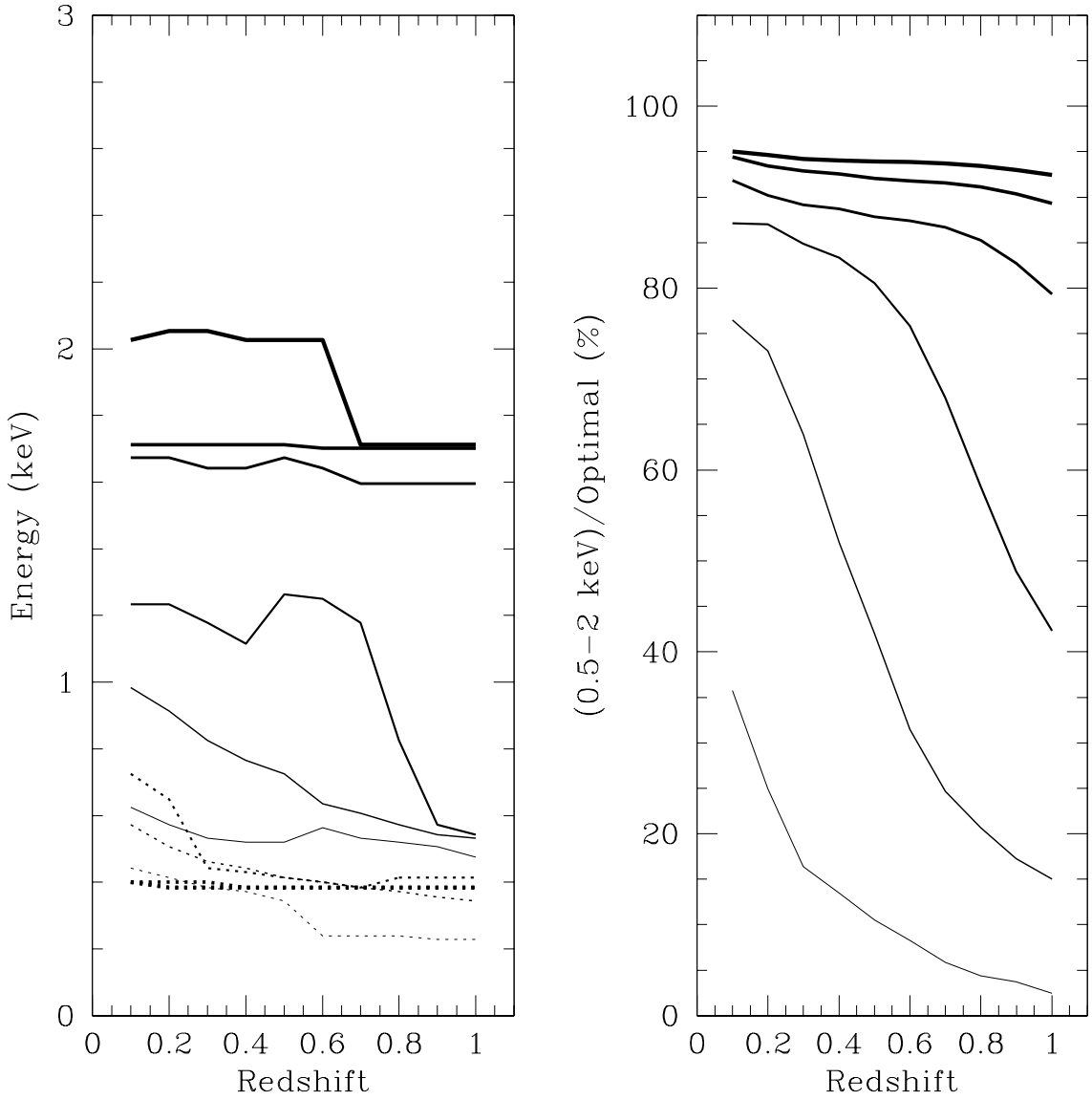

Fig. 3.— As for Figures 1 & 2, but for the XMM-Newton MOS instrument with a thin optical blocking filter

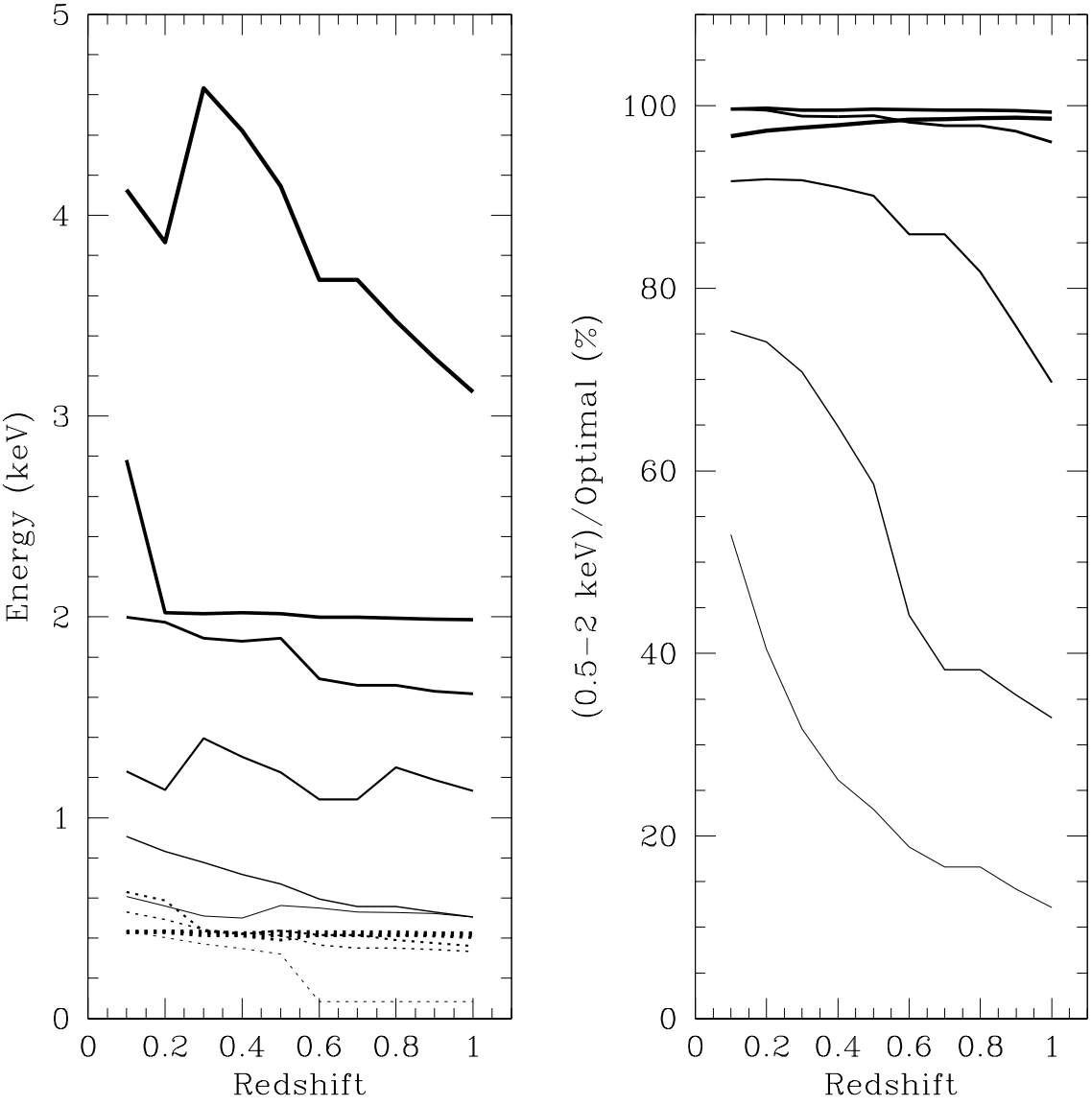

Fig. 4.— As for Figure 3, for the XMM-Newton PN instrument with a thin optical blocking filter